Polymer 51 (2010) 3512–3519

Contents lists available at ScienceDirect

Polymer

journal homepage: www.elsevier.com/locate/polymer

Mechanistic study of the formation of amphiphilic core–shell particles by grafting methyl methacrylate from polyethylenimine through emulsion polymerization

Kin Man Ho [a], Wei Ying Li [a], Cheng Hao Lee [a], Chun Ho Yam [a], Robert G. Gilbert [b], Pei Li [a,*]

[a] Department of Applied Biology and Chemical Technology, The Hong Kong Polytechnic University, Hung Hom, Kowloon, PR China
[b] CNAFS/LCAFS, University of Queensland, Brisbane, Queensland 4072, Australia

ARTICLE INFO

Article history:
Received 16 March 2010
Received in revised form
14 May 2010
Accepted 19 May 2010
Available online 2 June 2010

Keywords:
Polyethylenimine
Graft polymerization
Amphiphilic core–shell particles

ABSTRACT

The mechanism for the formation of amphiphilic core–shell particles in water is elucidated via a kinetic study of semi-batch polymerization of methyl methacrylate (MMA) grafted from polyethylenimine (PEI) initiated with *tert*-butyl hydroperoxide in an emulsion polymerization. The monomer conversion, the polymerization kinetics, the particle size, the particle number density, the poly(methyl methacrylate) (PMMA) core diameter, the percentage of unbound PEI, and the grafting efficiency of PMMA were determined at various times during the polymerization. The particle number density and the percentage of unbound PEI were almost independent of the controllable variables. The particle sizes and the core diameters increased with each consecutive batch of monomer addition, while the grafting efficiency of PMMA decreased. These data supported the hypothesis that the PEI-*g*-PMMA graft copolymers were formed early in the polymerization and later self-assembled to a new phase, micellar microdomains. These microdomains act as loci for subsequent MMA polymerization as the monomer is fed into the reaction, without subsequent formation of new particles. The size of the resulting highly uniform core–shell particles (99–147 nm) can be controlled by choosing the amount of monomer charged. Thus, this polymerization method is viable for a large scale production of core–shell particles with high solids content.

1. Introduction

Core–shell polymeric particles that consist of two or more very different chemical components and have particle diameters in nano- to micro-size ranges often exhibit improved physical and chemical properties over their single-component counterparts in applications as diverse as biomedicine and surface coatings. In particular, amphiphilic particles that consist of well-defined hydrophobic cores and hydrophilic shells have attracted much attention because of their potential applications in diagnostics, bio-separation, drug delivery, gene therapy, enzyme immobilization, coatings, and catalysis [1–3]. They are also of interest from a fundamental point of view in colloid and interface science [4–6].

Various synthetic approaches have been reported to synthesize amphiphilic core–shell particles based on polymerization and assembly methods. They include the following: (1) Graft copolymerization of a hydrophilic monomer onto a reactive seeded particle ("grafting from") via either conventional or living radical polymerization, producing *brush-like* particles [7–10]. (2) Copolymerization of a reactive macro-monomer with a hydrophobic monomer, producing *corona* particles [11]. (3) Emulsion polymerization in the presence of block copolymer [12,13] or comb-like copolymer [14] containing controlled free radicals moieties, producing *onion-like* particles. (4) Ab initio emulsion polymerization by self-assembly using controlled radical polymerization, producing particles containing two or more layers [15]. (5) Self-assembly of amphiphilic block copolymers followed by crosslinking the core or shell via covalent or ionic bonding, producing *knedel-like* nanoparticles [16–20]. (6) Stepwise deposition of polyelectrolytes onto charged particle surface [21,22], producing *raspberry-like* particles.

We have developed another route to synthesize well-defined, amphiphilic core–shell particles and hydrophilic microgels [23–26], based on the aqueous-phase redox reaction between *tert*-butyl hydroperoxide (TBHP) and amine functional groups of a water-soluble polymer. Initiation comes about when the amine-containing water-soluble polymers interact with a small amount of TBHP in water (70–80 °C being a convenient temperature) to generate free radicals on the amine nitrogen atoms. These radicals subsequently initiate the graft polymerization of the hydrophobic

* Corresponding author. Tel.: +852 2766 5616; fax: +852 2364 9932.
E-mail address: bcpeili@polyu.edu.hk (P. Li).

0032-3861/$ – see front matter © 2010 Elsevier Ltd. All rights reserved.
doi:10.1016/j.polymer.2010.05.035

monomer when the latter is fed into the vessel in a controlled way. The *tert*-butoxy radicals so generated can either initiate the homopolymerization of the monomer or abstract hydrogen from the backbone of the amine-containing polymer. The amphiphilic macroradicals generated *in situ* can self-assemble to form polymeric micelle-like microdomains, which can become loci for the subsequent polymerization of the monomer: a type of emulsion polymerization. Well-defined amphiphilic core–shell particles with diameters between 50 and 300 nm, thus can be produced in the absence of surfactant.

Although this method has proven to be effective in the synthesis of the amphiphilic core–shell particles, the particle formation mechanism is still not well understood. The objectives of this research are to elucidate the mechanism of the core–shell particle formation in a semi-batch polymerization, which could subsequently be used to achieve high-solids synthesis. The controlled monomer feed allows us to control exothermicity of the polymerization, copolymer composition and distribution, as well as particle morphology.

2. Experimental section

2.1. Materials

Branched PEI (50% solution in water, $\overline{M}_n \sim 60{,}000$ g mol^{-1}; $\overline{M}_w \sim 750{,}000$ g mol^{-1}) from Aldrich was used as received. Methyl methacrylate (MMA, Aldrich) was purified by washing three times with 10% w/w sodium hydroxide solution (MMA to NaOH volume ratio = 10: 1), followed by repeated washing with deionized water (MMA to water volume ratio = 5: 1) until the pH of the water layer dropped to 7. It was further purified by a vacuum distillation prior to use. *Tert*-Butyl hydroperoxide (70% w/w solution in water) was obtained from Acros, and used as received. Freshly deionized and distilled water or Milli-Q water was used as the dispersion medium.

2.2. Semi-batch emulsion polymerizations

Amphiphilic PMMA/PEI particles were prepared using the recipe shown in Table 1. A typical procedure is described as follows: Branched PEI (2.036 g) was first dissolved in water, and the resulting solution was then adjusted to pH 7.0 by adding 2 M HCl solution. The PEI solution was transferred into a water-jacketed flask equipped with a condenser, a thermocouple, a magnetic stirrer, and a nitrogen inlet, then stirred at 600 rpm and purged with nitrogen for 20 min at 80 °C. Purified MMA monomer (2.0 g) was subsequently added to the PEI solution. After mixing for 5 min, a dilute TBHP solution (1 mL, 100 mM) was charged to the stirred mixture to initiate the polymerization. Afterwards, different amounts of MMA (Table 1) were charged to the reactor at the same interval (20 min). Samples (1–2 g) were withdrawn from the reactor using a hypodermic syringe through a septum, and were immediately placed in liquid nitrogen. The instantaneous conversion of each batch reaction was determined gravimetrically, as the percentage conversion of a total monomer added up to that point in time (including the monomer used in the seed stage).

Table 1
Recipe used for the semi-batch emulsion polymerization.[a]

Ingredient	Amounts
Water	89.50
PEI•HCl	2.98 g
TBHP	1 mM
MMA	2, 2, 1, 1, 1, 1 g for each batch addition (total 8 g)
Reaction time	Batch addition: 20, 40, 60, 80, 100 min

[a] Total solution weight = 100 g; solids content = 10%; MMA:PEI = 4:1 (w/w); 80 °C; 3 h.

2.3. Determination of the percentage of unbound PEI

The unbound PEI was determined by collecting all supernatants from each repeated centrifugation, decantation, and redispersion cycle of the latex dispersion. The free PEI obtained from a combined supernatant was then titrated with a NaOH solution and their pH and conductivity changes were monitored by pH and conductometric titrations (ThermoOrion 555A integrated pH/conductivity meter). Since the conductivity measurement is sensitive to the free ions present in the solution, but insensitive to the deprotonation of the polyelectrolyte (e.g., PEI), excess NaOH ions may cause a dramatic increase in conductivity of the solution. Thus, the equivalence point was determined as the pH value at which a dramatic increase in conductivity of the solution began. A PEI calibration cruve was established according to the following procedure. Various amounts of PEI solution (50% w/w) were dissolved in water (40 mL), and their pH values were adjusted to 7.0 using a 2 M HCl solution. The resulting PEI solutions were then titrated with a NaOH solution (0.025 M) at room temperature under nitrogen atmosphere to an equivalence point, which is defined as the pH value at which the amount of hydroxide ions completely deprotonate all the protonated amino groups of PEI. Figure S1 shows the calibration curve of PEI solution. The percentage of unbound PEI was then determined with reference to the calibration curve.

2.4. Determination of PMMA grafting efficiency

The grafting efficiency is defined as the weight of grafted PMMA divided by the weight of total polymerized MMA (Eq. (1)).

$$\text{Grafting efficiency} = \left(\frac{\text{weight of grafted PMMA}}{\text{weight of total polymerized MMA}}\right) \times 100\% \quad (1)$$

The weight of grafted PMMA is obtained by subtracting the weight of PMMA homopolymer from the weight of total polymerized MMA. The PMMA homopolymer was isolated by the solvent evaporation method [27]. A typical procedure is described as follows. Freeze-dried PMMA/PEI particles (0.05 g) were first mixed with 5 mL of dichloromethane (DCM). The suspension was gently stirred at 150 rpm at room temperature for 3 h to extract the PMMA homopolymer from the cores. Deionized water was then added dropwise (4.8 mL/min) to the DCM solution up to a DCM to water volume ratio of 3:7. The resulting DCM/water mixture was subsequently stirred at 150 rpm with a magnetic stirrer. During this process, the solution temperature was thermostated by water circulation using a temperature-controlled circulator (IMT InMedtec Co.) at 25 °C. After the DCM had completely evaporated, the insoluble PMMA homopolymers (white solids) in water were simply removed by filtration. After drying the polymer in a vacuum oven, the chemical structure of the solids was identified by Fourier-Transform Infrared (FT-IR) spectroscopy (Nicolet Avatar 360 FT-IR spectrophotometer) using KBr disks, and confirmed to be PMMA homopolymer.

2.5. Measurements and characterization

The ^{1}H NMR spectral and relaxation (T_1) measurements were carried out on a Bruker Advance DPX-400 FT-NMR spectrometer, operating at the Larmor frequency of 400.13 MHz per proton. A 30°

pulse of 9.5 μs and an acquisition delay of 2 s were used for ^{1}H spectral accumulation. A "π-τ-π/2–acquisition" inversion recovery sequence was used for T_1 measurements and the FT data were fitted using the online Bruker software *SIMFIT*.

To determine the volume-average diameter and morphology of the particles in each batch, samples were withdrawn from reaction vessel at every 20 min prior to the addition of next batch of monomer. They were then purified by repeated centrifugation, decantation and redispersion, followed by characterization with transmission electron microscopy (TEM) using a JEOL 100 CXII TEM at an accelerating voltage of 100 kV. The TEM sample was prepared by wetting a carbon-coated copper grid with a small drop of dilute particle dispersion in water (10 μL, 300 ppm). Upon drying, the particles were stained with a small drop of 0.5% w/w phosphotungstic acid solution (PTA) for 30 s, and then dried at room temperature before analysis. All TEM images were taken in a bright-field mode. Statistical analyses of particle size data including volume-average diameter (D_v), weight-average (D_w) and number-average (D_n) were obtained by counting at least 100 particles from TEM images, and the results are provided in Table S1 (Supporting Information).

The hydrodynamic diameters $\langle D_h \rangle$ of amphiphilic core–shell particles were measured with a Malvern Zetasizer 3000HS (Malvern, UK) using a He–Ne laser at a wavelength of 632.8 nm. The measurements were performed at 25 °C with a fixed angle of 90°. Sample concentrations were between 100 and 300 ppm.

The number of particles per unit volume of aqueous phase, N_p, was calculated from Eq. (2) [28]:

$$Np = \frac{6m_p}{\pi D_v^3 d_p} \tag{2}$$

where m_P is the total mass of polymer (per unit volume of aqueous phase) in the system and d_p is the density of PMMA (1.178 g cm^{-3}). The average number of free radicals per latex particle ($\bar{n}$) was calculated from Eq. (3) [28]:

$$\bar{n} = \frac{R_p N_A}{k_p C_p N_p} \tag{3}$$

where R_p is the initial rate of polymerization (which was determined from the initial slope of the mass of polymers produced as a function of time in each batch polymerization), N_A is the Avogadro constant, k_p is the propagation rate coefficient (k_p = 1311 L mol^{-1} s^{-1} at 80 °C was used, from the Arrhenius parameters given in Beuermann et al. [29]), and C_p is the concentration of monomer in the polymer particles.

When the system is under flooded conditions (monomer droplets present), then C_p has its equilibrium saturated value (C_p^{sat}) of 6.6 M [30]. When the system is under starved conditions (no monomer droplets present), then the calculation of C_p needs to take into account of the significant solubility of monomer in the water phase, C_w, as Eqs. (4–7). The saturated water solubility of MMA is 0.15 M [30]. One has:

$$Cw = \left(\frac{m_{M,w}}{M_0}\right)\frac{d_w}{m_w} \tag{4}$$

where $m_{M,w}$ is the mass of monomer in the water phase in the system, d_w is density of water and M_0 is the molecular weight of monomer. The non-ideal partitioning of monomer between particle and water phases is taken to obey the empirical relation for MMA [30]:

$$\frac{C_w}{C_{w^{sat}}} = \left[\frac{C_p}{C_{p^{sat}}}\right]^{0.6} \tag{5}$$

Conservation of mass gives Eq. (6) (assuming that no monomer droplets are present):

$$m_{M,p} = m_M - m_{M,w} = C_p\left(\frac{m_p}{d_p} + \frac{m_{M,p}}{d_M}\right)M_0 \tag{6}$$

where $m_{M,p}$ is the mass of monomer in the particles, d_M is the density of monomer, d_P is the density of polymer and mP is obtained from the conversion data.

Combining Eqs. (5) and (6) gives Eq. (7).

$$\frac{m_{M,w}}{M_0 C_{w^{sat}}} = \frac{1}{(C_{p^{sat}})^{0.6}}\left[\frac{m_M m_{M,w}}{M_0}\left(\frac{d_P}{m_P} + \frac{d_M}{m_M m_{M,w}}\right)\right]^{0.6} \tag{7}$$

This is a non-linear relation for $m_{M,w}$, which is solved numerically (e.g. using the 'solver' function in Excel). The value of C_p is then obtained from Equation (6).

To determined whether or not the system is flooded, Cp is evaluated as described; if the value so obtained exceeds the saturated value the system is flooded, and if Cp < Cpsat, then the system is starved. This is more precise than experimental techniques such as trying to see if monomer droplets are present, because these are hard to detect if the system is close to flooded conditions.

3. Results and discussion

3.1. Synthesis of PMMA/PEI core–shell particles via semi-batch polymerization

During the semi-batch polymerization, four possible reactions may take place, as illustrated in Fig. 1 [23]. (1) The TBHP (*t*-BuOOH) initially interacts with amino group of the polymer backbone, forming redox pair. One electron is then transferred from an amine nitrogen to *t*-BuOOH, resulting in the formation of a nitrogen cation radical and a *tert*-butoxy (*t*-BuO•) radical. After losing a proton, the amino radical can initiate polymerization of MMA dissolved in water, generating amphiphilic PEI-*g*-PMMA macroradical. (2) The *t*-BuO• radical can initiate the homopolymerization of MMA. (3) The *t*-BuO• radical may also abstract hydrogen atom from the backbone of the polymer to form macroradical. (4) The amphiphilic macroradicals generated *in situ* are able to self-assemble to form micelle-like microdomains, thus facilitating the polymerization of MMA inside the microdomains. This is similar to the mechanism of conventional emulsion polymerization. As a result, amphiphilic core–shell particles, which consist of both PMMA grafts and PMMA homopolymers are produced in the absence of surfactants.

To elucidate the polymerization mechanism, syntheses of PMMA/PEI core–shell particles were conducted at 80 °C, using the recipe shown in Table 1. The reaction temperature was monitored online. Fig. 2 shows that when the graft polymerization of MMA from PEI was initiated with TBHP, temperature of the reaction mixture increased rapidly by 1–2 °C, then quickly dropped back to the starting temperature.

Fig. 2 also shows that increasing in temperature after each batch addition depends on the amount of monomer added. Smaller amounts of monomer resulted in smaller temperature changes, suggesting that the system was running in different monomer saturation conditions (as supported by the calculated Cp in Table 2). Another observation from this temperature/conversion profile is that high MMA instantaneous conversions (79–89%) could be achieved without the need to charge additional initiator in each batch polymerization. These results suggest that active radicals are able to be generated for at least 3 h, allowing sequential polymerization without adding extra initiator. This effect may be attributed

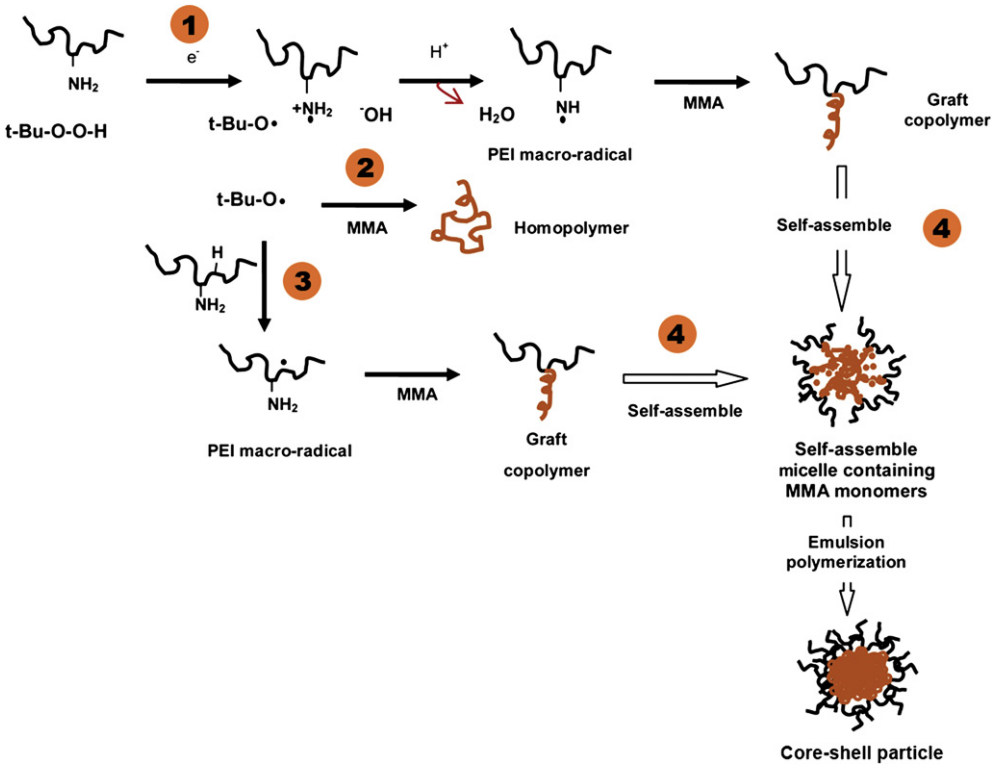

Fig. 1. Mechanism of the graft polymerization of MMA from a water-soluble polymer containing amino groups.

to TBHP undergoing thermal dissociation and low radical termination because of the compartmentalization effect inside particles.

The rate of reaction (R_p) is obtained from the mass of PMMA polymer produced as a function of time calculated from the average slopes in the initial stage of each batch reaction (Fig. 3). These rates are shown in Table 2. All apparent C_p values calculated from mass conservation and partitioning, Eqs. (4)–(7), were actually above the saturation value, indicating that the system is flooded (monomer droplets are present), i.e. C_p is the saturation value of 6.6 M. Together with the data of particle size (see next sub-section), these rates can be converted to $\bar{n}$ (Table 2). Results indicate that $\bar{n}$ steadily decreases throughout the reaction.

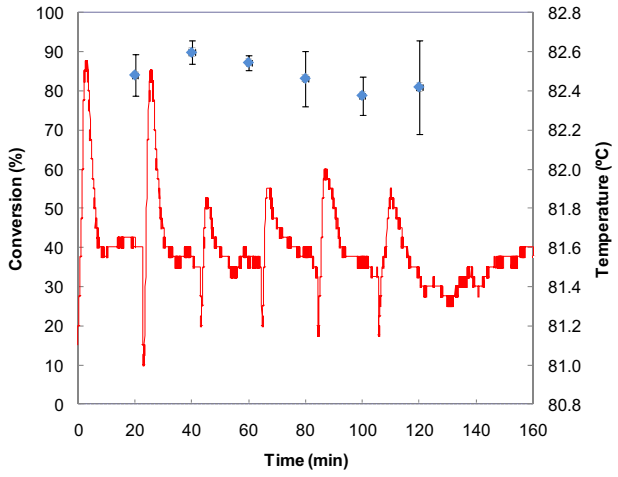

Fig. 2. Line: online temperature measurement of reaction temperature for the semi-batch polymerization of MMA from PEI initiated with TBHP at 80 °C. Points: instantaneous monomer conversion as a function of reaction time (each datum is an average of three repeated experiments under the same conditions).

MMA emulsion polymerization follows pseudo-bulk rather than zero-one kinetics [30], and $\bar{n}$ can assume any value. The $\bar{n}$ values found here are in the range between 0.24 and 0.83, which are not unusual for MMA seeded emulsion polymerization [30]. While there is good quantitative understanding of MMA emulsion polymerization kinetics [31], the present system involves an unknown initiation rate: that of the PEI/TBHP redox initiation. Moreover, the presence of PEI means that there is also the possibility of an additional radical loss mechanism: the "mid-chain radical" effect, resulting in a radical which is slow to propagate but quick to terminate as a result of substantial radical loss [32–34]. This effect occurs when an electrosterically stabilized water-soluble polymer [e.g., poly(acrylic acid) and poly(ethylene glycol)] that contains a labile hydrogen is used as a stabilizer ('hairy layer') in emulsion polymerization system. In our system, since the PEI molecule contains a labile hydrogen (–$CH_2\underline{CH_2}$–NH–) adjacent to the secondary amine [35], mid-chain radicals (–$CH_2\dot{C}H$–NH–) can be formed by radical abstraction on the PEI backbone during polymerization, causing a radical loss. The two aspects of the emulsion polymerization of MMA in the presence of PEI that are hard to quantify, viz., the unknown radical generation rate and the unknown rate of abstraction of a labile hydrogen, make it impossible to model the values of $\bar{n}$ without additional data on these processes.

3.2. Particle size and number of particles

Secondary nucleation, which often results in new particle formation, can readily occur in a semi-batch seeded emulsion polymerization. It will lead to an increase in number of particles, and usually a decrease in average particle size. To study this effect, particle sizes and their size distributions were measured during polymerization by withdrawing samples from the reaction vessel every 20 min prior to the addition of next batch of monomer (Table S1, Supporting Information). Their particle morphologies were

Table 2
Semi-batch polymerization of MMA from PEI at different polymerization time with respect to their initial rates of polymerization (R_p), calculated average number of free radicals per latex particle ($\bar{n}$) and apparent C_p values.

Batch	1	2	3	4	5	6
Time period (min)	0–20	20–40	40–60	60–80	80–100	100–120
S_r (%)[a]	149	149	75	75	75	75
R_p (10^{-4} mol dm^{-3} s^{-1})[b]	–	13.23 ± 0.22	4.49 ± 0.13	2.98 ± 0.14	2.30 ± 0.045*	3.11 ± 0.48*
Apparent C_p (M)[c]	–	12.0	8.9	9.3	9.9	10.8
N_p (10^{16} dm^{-3})		6.12 ± 1.07	6.03 ± 1.43	5.66 ± 1.34	4.39 ± 1.16	4.62 ± 1.33
$\bar{n}$[d]		0.83 ± 0.28	0.39 ± 0.19	0.26 ± 0.07	0.24 ± 0.04	0.30 ± 0.13

[a] The S_r is the monomer saturation ratio which defines as the concentration of monomer in water with reference to saturation concentration of MMA in water (1.5% w/w). At $S_r < 100\%$, MMA completely dissolves into water; while at $S_r > 100\%$, the excess MMA can't dissolve in water resulting in separating into monomer droplet phase.
[b] R_p was determined from the initial slope of the mass of polymers formed in each batch of polymerization as shown in Fig. 3 (*Note that the derived R_p has a relatively larger error in the 5th and 6th batches, probably because a small amount of particle aggregation starts to appear in these, causing fluctuation of gravimetric data (with 9–15% errors)).
[c] Apparent C_p values were calculated from Eqs. (4)–(7) (assuming no monomer droplets are present).
[d] $\bar{n}$ is calculated from Eq. (3).

observed with TEM. All samples were stained with a 0.5% phosphotungstic acid (PTA) solution for an appropriate time in order to enhance the contrast between PMMA cores and PEI shells. Since hydrophilic PEI molecules can form complexes with negatively charged PTA molecules, this treatment results in a higher electron density in the PEI region than that of the PMMA region. Fig. 4 shows the TEM micrographs of PMMA/PEI particles produced at different stages of polymerization. The darker shells indicate the presence of PEI/PTA complexes due to stronger electron scattering, while the lighter cores are the PMMA cores. All the images clearly reveal core–shell nanostructures, where PMMA cores (lighter region) are coated with PEI shells (darker region).

Statistical analysis of the diameters of the particles in these TEM images gives volume-average diameters (D_v), whence the number of particles (N_p) can be calculated using Eq. (2). Fig. 5 shows the relation between D_v and N_p versus time at different stages of polymerization. In the first batch reaction (20 min), seed particles with a D_v of 99 nm were formed. Subsequent additions of five batches of monomers resulted in increasing particle diameters from 99 to 147 nm, while the numbers of particles were almost the same within experimental uncertainty. These results suggest that the polymerization of monomer in each batch of monomer addition takes place within the seed particles. There is no new nucleation apparent between 20 and 80 min. There may possibly be a very slight decrease in the number of particles per unit volume of the continuous phase, but this is within experimental uncertainty. This could be explained by a small amount of particle aggregation. To substantiate the hypothesis about no new nucleation occurring, we have calculated the theoretical mass of polymers based on size data using mass conservation equation (i.e., mass = assumed number density × polymer density × average particle volume), and then compared with the mass of polymers obtained from gravimetry data in different stages. If there is no new nucleation (assuming that the number density was constant in all stages), the theoretical mass of calculated polymers should be close to the mass obtained from the gravimetry data. Assuming that the number density is 5.2×10^{16} L^{-1} and using a volume-average diameter in each stage for calculation, the theoretical mass of polymers is obtained (Figure S2, Supporting Information). The results show good agreement with the mass of PMMA produced from gravimetric data (within experimental uncertainty) between 20 and 80 min, suggesting that the particle growth (increase in particle diameters) is indeed due to the increase in mass of PMMA polymers, and there are almost no newly formed particles. However, for the reaction time between 80 and 120 min, the mass of PMMA calculated from mass conservation equation shows positive deviation from that obtained from gravimetric data. These results suggest that the numbers of particles are overestimated, consistent with the decrease in number of particles between 80 and 120 min.

3.3. Mechanism of particle growth

On the basis of above results, it is proposed that the core–shell seed particles are initially formed via formation of amphiphilic graft copolymers, followed by their *in situ* self-assembly to generate micelle-like microdomains. After the first batch reaction, the reaction mixture mainly contains amphiphilic seed particles and unreacted PEI. When the second batch of MMA is charged into the mixture, there are two possible polymerization pathways: 1) The MMA molecules are polymerized by the PEI macroradicals in water to form new graft copolymeric radicals. The resulting graft copolymers could either enter into the existing seed particles or self-assemble to form new micelle-like microdomains, thus leading to secondary particle formation. 2) The MMA monomer quickly diffuses into the seed particles, and is polymerized inside the particles. In order to elucidate the mechanism of particle growth, the percentage of unbound PEI and the grafting efficiency of PMMA in each batch prior to the next addition of monomer were systemically investigated.

3.3.1. Kinetics of graft copolymerization

One possible reaction pathway is that the newly added MMA monomers are polymerized with PEI macroradicals in water, generating new PEI-*g*-PMMA copolymers which may enter the existing seed particles. If the polymerization occurs in this way, it is expected that the amount of free PEI in water should decrease after each batch of polymerization. To investigate this, we purposely added an excess amount of PEI in the polymerization mixture so

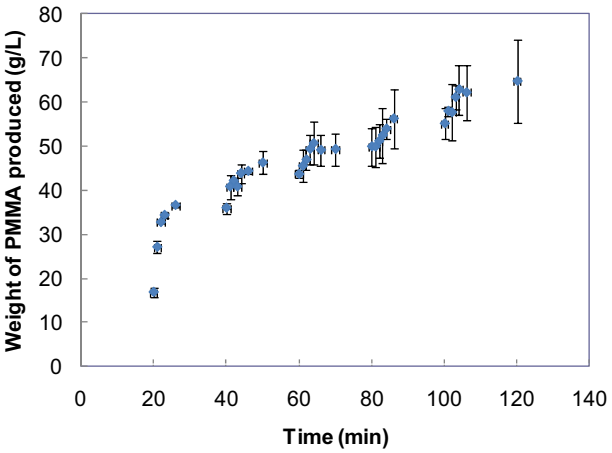

Fig. 3. Mass of PMMA produced as a function of reaction time, for sequential monomer addition at 20, 40, 60, 80, 100 min (each datum is an average of three repeated experiments under the same conditions).

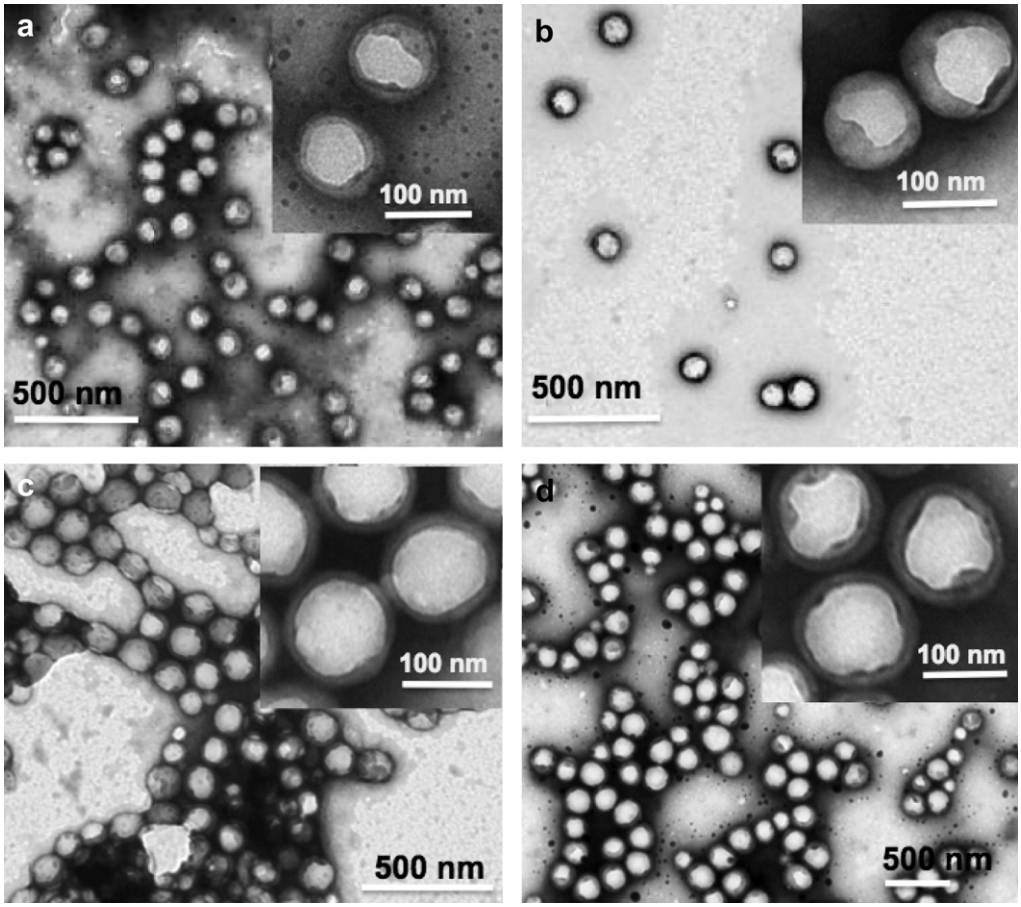

Fig. 4. TEM images of core–shell particles generated at different stages of polymerization: (a) 20 min ($D_v = 99$ nm); (b) 40 min ($D_v = 117$ nm); (c) 80 min ($D_v = 129$ nm); (d) 120 min ($D_v = 147$ nm). All purified samples were stained with a 0.5% PTA solution for 30 s prior to TEM measurement.

that the changes in the amount of the ungrafted PEI in each batch polymerization could be accurately determined through pH and conductometric titrations of supernatants. The supernatants were collected from four repeat cycles of centrifugation, decantation and redispersion of the resulting centrifuged pellet. To ensure that the supernatant did not contain the PEI-*g*-PMMA copolymers, which may complicate the result of the percentage of unbound PEI, the collected supernatants were analyzed with ^{1}H NMR spectroscopy, which confirmed that there were no PEI-*g*-PMMA graft copolymers; only free PEI was detected. Fig. 6 shows the percentages of unbound PEI during the polymerization. For the first batch reaction, the percentages of unbound PEI were difficult to determine because the seed particles were too small to be completely separated even under a high centrifugation speed (18000 rpm). In the subsequent batches of reactions, the percentages of unbound PEI varied from 38 to 42%. Such a small variation suggests that once the seed particles are formed after the first batch of polymerization, the remaining PEI molecules almost do not react with newly added

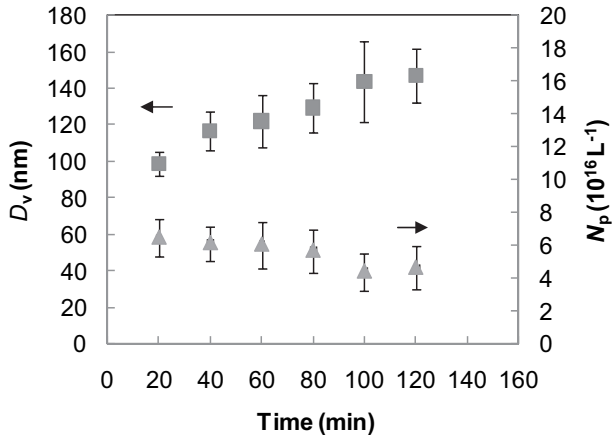

Fig. 5. Volume-average diameter (D_v) and number of particles (N_p) at different stages of monomer addition. (■) D_v and (▲) N_p.

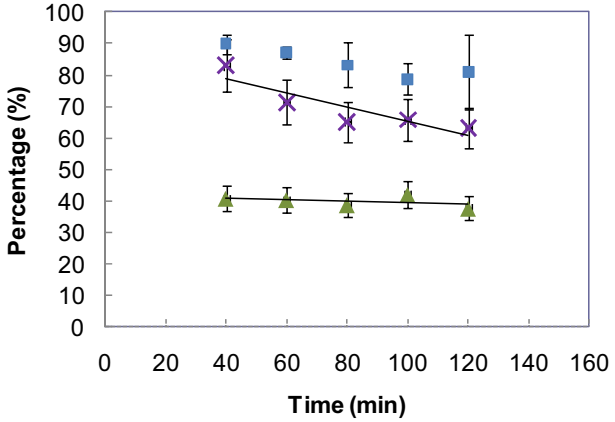

Fig. 6. Kinetic study of semi-batch polymerization of MMA from PEI: (▲) percentage of unbound PEI (line: linear fit); (×) PMMA grafting efficiencies (line: linear fit) and (■) instantaneous conversion in each batch of polymerization.

MMA monomer to form PEI-*g*-PMMA copolymers in subsequent batches of monomer addition. These results suggest that the first possible polymerization pathway is unlikely. This phenomenon may be due to the fact that when the PEI-*g*-PMMA copolymers formed *in situ* reach their hydrophilic/hydrophobic balance, they self-assemble to form micelle-like microdomains [23]. Once the microdomains are formed, most newly formed *tert*-butoxy radicals will be located in the cores of the particles because of their high entry rates and capture efficiency [36]. When MMA is added, the usual emulsion polymerization mechanistic reasons for polymerization occurs within the seed particles: either they are initiated by the *tert*-butoxy radicals in the core, or if they start to polymerize in the aqueous phase, they rapidly reach a critical degree of polymerization (usually denoted j_{crit}) to undergo a coil–globule transition and then enter the particles. Formation of mid-chain radicals later in the polymerization may result in somewhat lower rates, because such radicals are slow to propagate but quick to terminate.

3.3.2. Kinetics of homopolymerization and loci of seeded polymerization

To further understand the polymerization kinetics and loci of the seeded polymerization, polymerization in the presence of the seed particles was investigated. It was assumed that when the MMA monomer was fed into the reaction mixture containing a large number of seed particles, monomer could rapidly diffuse into the seed particles, and be polymerized inside the particles through either graft copolymerization or homopolymerization. The PMMA grafting efficiency, which is defined as the amount of grafted PMMA divided by the amount of total MMA polymerized, was investigated by isolation of ungrafted PMMA polymers using the solvent evaporation method, as described in the experimental section. The FT-IR spectra of the isolated polymers showed characteristic peaks of PMMA [stretching vibrations of C=O (1731 cm^{-1}), and C–O of ester (1000–1200 cm^{-1})], but not the characteristic peak of PEI [N–H stretching of primary amine (3300–3400 cm^{-1})) (Figure S3, Supporting Information). These results suggest that the isolated polymer was the PMMA homopolymer.

Fig. 6 also shows that monomer conversions in all batch polymerizations were quite high (>80%); however, the grafting efficiencies varied. The highest grafting efficiency was achieved at the second batch polymerization (83%), and then dropped to 71% at the third batch. The grafting efficiencies for the 4th, 5th, and 6th batches were comparable, ranging from 62 to 66%. The high grafting efficiency in the second batch polymerization suggests that the graft copolymerization is a dominant pathway in the beginning, generating amphiphilic graft copolymers, followed by their self-assembly to generate seed particles. For the subsequent batch polymerizations, homopolymerization of MMA inside the seed particles was a preferential pathway for particle growth, resulting in the increase in homopolymer formation. These results are consistent with the TEM micrographs, in which the increase in particle size is mainly from the growth of particle cores.

3.4. Proposed mechanism for particle formation and growth

Based on the above studies, we propose that there are five key stages for particle formation and growth of amphiphilic core–shell particles: (1) The PEI-*g*-PMMA copolymers are first generated *in situ* through graft polymerization of MMA from PEI via redox initiation between amino groups and the TBHP in water; (2) Those graft copolymers which have appropriate hydrophobic/hydrophilic balance can self-assemble to form micelle-like microdomains. At this stage, these microdomains contain amphiphilic graft copolymeric radicals; (3) The microdomains then create a hydrophobic interior to drive *tert*-butoxy radicals and MMA monomers into the micellar cores. (4) As a result, the MMA is polymerized therein via both graft polymerization and homopolymerization pathways, resulting in the formation of amphiphilic seed particles. (5) When a new batch of monomers is charged to the reaction mixture, which contains seed particles and free PEI, monomer rapidly diffuses and swells the hydrophobic cores of existing seed particles, instead of reacting with free PEI in water to form new PEI-*g*-PMMA microdomains. Thus, almost no secondary particle formation occurs during the polymerization. All subsequent polymerization takes place in the interior of the particles.

4. Conclusions

The mechanism for the formation of amphiphilic core–shell polymeric particles in water has been elucidated through the kinetic study of semi-batch polymerization of MMA from PEI initiated by TBHP. The micelle-like microdomains, generated from self-assembly of PEI-*g*-PMMA graft copolymers, provide the main locus of polymerization. Once the seed particles are formed, newly added MMA is mainly polymerized inside the cores of the seed particles. Thus, almost no secondary particle formation is observed. With this technique, the exothermicity of polymerization can be controlled through the feed rate of added monomer. Thus this polymerization method is viable for a large scale production of core–shell particles with high solids content.

Acknowledgments

We gratefully acknowledge the Hong Kong Polytechnic University Postdoctoral Fellowship Scheme and University Research Grants Council of the Hong Kong SAR (PolyU 5013/06P) for financial support.

Appendix. Supplementary material

Supplementary data associated with this article can be found, in the online version, at doi:10.1016/j.polymer.2010.05.035.

References

[1] Kawaguchi H. Prog Polym Sci 2000;25:1171.
[2] Pichot C. Curr Opin Colloid Interf Sci 2004;9:213.
[3] Anstey J, F, Subramaniam N, Pham B, TT, Lu X, Monteiro M, J, Gilbert R, G. Macromol Symp 2000;150:73.
[4] Caruso F. Adv Mater 2001;13:11.
[5] Coen EM, Lyons RA, Gilbert RG. Macromolecules 1996;29:5128.
[6] Vorwerg L, Gilbert RG. Macromolecules 2000;33:6693.
[7] Tsuji S, Kawaguchi H. Langmuir 2004;20:2449.
[8] Kizhakkedathu JN, Norris-Jones R, Brooks DE. Macromolecules 2004;37:734.
[9] D'Agosto F, Hughes R, Charreyre M-T, Pichot C, Gilbert RG. Macromolecules 2003;36:621.
[10] D'Agosto F, Charreyre M, Pichot C, Gilbert R, G. J Polym Sci A Polym Chem 2003;41:1188.
[11] Basinska T, Slomkowski S, Kazmierski S, Dworak A, Chehimi M, M. J Polym Sci A Polym Chem 2004;42:615.
[12] Burguiere C, Pascual S, Bui C, Vairon J-P, Charleux B, Davis KA, et al. Macromolecules 2001;34:4439.
[13] Nicolas J, Ruzette A-V, Farcet C, Gérard P, Magnet S, Charleux B. Polymer 2007;48:7029.
[14] Save M, Manguian M, Chassenieux C, Charleux B. Macromolecules 2004;38:280.
[15] Ferguson CJ, Hughes RJ, Nguyen D, Pham BTT, Gilbert RG, Serelis AK, et al. Macromolecules 2005;38:2191.
[16] Zhang Q, Remsen EE, Wooley KL. J Am Chem Soc 2000;122:3642.
[17] Weaver JVM, Tang Y, Liu S, Iddon PD, Grigg R, Billingham NC, et al. Angew Chem Int Ed 2004;43:1389.
[18] Saito R. Macromolecules 2001;34:4299.
[19] Liu S, Armes SP. J Am Chem Soc 2001;123:9910.
[20] Cheng C, Qi K, Khoshdel E, Wooley KL. J Am Chem Soc 2006;128:6808.
[21] Quinn JF, Caruso F. Langmuir 2003;20:20.
[22] Khopade AJ, Caruso F. Langmuir 2003;19:6219.
[23] Li P, Zhu J, Sunintaboon P, Harris FW. Langmuir 2002;18:8641.

[24] Zhu J, Li P. J Polym Sci A Polym Chem 2003;41:3346.
[25] Leung MF, Zhu J, Harris FW, Li P. Macromol Rapid Commun 2004;25:1819.
[26] Li W, Li P. Macromol Rapid Commun 2007;28:2267.
[27] Sunintaboon P, Ho KM, Li P, Cheng SZD, Harris FW. J Am Chem Soc 2006;128:2168.
[28] Gilbert RG, Emulsion polymerization: a mechanistic approach London; 1995.
[29] Beuermann S, Buback M, Davis TP, Gilbert RG, Hutchinson RA, Kajiwara A, et al. Macromol Chem Phys 2000;201:1355.
[30] Ballard MJ, Napper DH, Gilbert RG. J Polym Sci Polym Chem Edn 1984;22:3225.
[31] van Berkel KY, Russell GT, Gilbert RG. Macromolecules 2005;38:3214.
[32] Thickett SC, Gilbert RG. Macromolecules 2006;39:6495.
[33] Thickett SC, Gaborieau M, Gilbert RG. Macromolecules 2007;40:4710.
[34] Thickett SC, Morrison B, Gilbert RG. Macromolecules 2008;41:3521.
[35] Xu D, Hong J, Sheng K, Li D, Yao S. Radiat Phys Chem 2007;76:1606.
[36] Lamb DJ, Fellows CM, Gilbert RG. Polymer 2005;46:7874.